A NEW APPROACH TO THE QUASAR FUNDAMENTAL PLANE

Rudolph Schild, Harvard Smithsonian Center for Astrophysics, Cambridge, MA 20138

Darryl Leiter, Visiting Scientist, NRAO, Charlottesville, VA 22901

ABSTRACT

Attempts to infer quasar masses from luminosities have consistently produced marginal results with scatter of a factor approximately 10 in the mass estimates. We show that for the MECO/Black-Hole model the luminosity is a function of a rotation parameter in addition to mass, which we take to be the a/M ratio in Eddington units from the MECO surface spin in units of Hz. Thus we define a fundamental plane to define the relationship of mass to observable fundamental parameters.We show that the scatter in the relationship of mass to luminosity involves other observable parameters related to rotation and the accretion rate. We also extend the discussion of quasar spectral states with the definition of the Radio Loud - Very High State (RL- VHS) to the previously discussed Radio Loud - Low Hard State (RL - LHS) and the Radio Quiet - High Soft State (RQ - HSS).

I. INTRODUCTION

Unique microlensing observations of quasar Q0957 in a radio loud low hard state and quasar Q2237 in a radio quiet spectral high soft state have permitted a detailed reconstruction of their internal structures emitting radiation (Schild, Leiter, and Robertson; Astron. Journ, v132, p140, (2006); Astron. Journ.,v135, p947, (2008)).

The internal structures, observed within these two quasars in different spectral states, have been found to be similar to the features seen in accretion flows into young stellar objects which contain central compact objects which possess intrinsically anchored magnetic moments. The existence of intrinsic magnetic moments within the central super massive compact objects inside of these two quasars were observationally supported by the fact that: a) the inner accretion disk of the radio loud quasar was truncated at a very large radius by a very thin hot inner ring surrounding a large empty interior region and, b) both the radio loud and the radio quiet quasars contained elliptical Elvis outflow structures, at radial distances about ten times further out, which had very wide opening angles greater than 60 degrees. On this basis we concluded that in these two quasars we were observing the physical effects associated with the presence of intrinsically magnetic, highly red shifted central compact objects in these quasars which cannot be black holes because astrophysical black holes cannot possess observable intrinsic magnetic moments.

Instead the central compact objects in these appeared to be "Magnetospheric Eternally Collapsing Objects" (MECO) which are permitted in the framework of the Einstein-Maxwell equations when solved within the context of Quantum Electrodynamic plasma physics, (Robertson and Leiter, ApJ, v565, p447, (2002); ApJL, v596, p203, (2003); MNRAS, v350, p1391, (2004)). MECO can form by DRAFT PAPER #1 1/15/2009 2 the same gravitational collapse process believed to result in black holes but due to internally generated synchrotron radiation pressure, which becomes trapped inside of the photon sphere, they become Eddington limited and secularly stable at a very high red shift and are thus prevented from collapsing through their event horizons. Due to the extreme red shifts of the surface radiation emitted from the MECO Eddington limited surface, their intrinsic surface radiations are too faint to be easily detected at astronomical distances. However in quasars we find that MECO can be observationally distinguished from black holes primarily by their ability to exhibit the observable effects of their intrinsic magnetic moments on their quasar accretion disk environments.

In this paper we demonstrate how the combination of the MECO model with the empirical Kaspi correlation, between the size of the broad line region of a Quasar and its bolometric Eddington ratio, leads us to the MECO-Quasar Fundamental Plane (MQFP) which determines the specific angular momentum (a/M) of the MECO-Quasar in terms of the quasar mass and the quasar bolometric Eddington ratio.

II. THE MECO-QUASAR FUNDAMENTAL PLANE (MQFP)

It is well known that bi-conic elliptical Elvis coronal outflows can be generated, by compact astrophysical objects which have accretion disks, by the combined presence of two physical processes:

(a) magnetic reconnection effects which can generate upward flows from an accretion disk just inside of the outer light cylinder of a central compact magnetic object contained within the accretion disk (Uzdensky 2002, 2006; Spitovsky 2006), and,

(b) optical line driving forces, associated with the presence of strong ultraviolet luminosity emitted from the inner region of a hot accretion disk, surrounding the central compact magnetic object, which can act on the magnetic reconnection generated upward flows just inside of the outer light cylinder and there create the bi-conic Elvis outflow structures (Elvis 2000, 2003, 2006).

It is interesting to note that above described physical scenario can automatically be applied to the MECO-quasar model (Schild, Leiter, Robertson, 2006, 2008) for the following reasons:

a) the intrinsic rotating magnetic field of the central compact MECO generates a vertical up-flow of plasma above the accretion disk by magnetic reconnection effects which occur just inside of the outer light cylinder of the MECO and,

b) for the high values of the Eddington ratios associated with quasars, the accretion disk at the magnetospheric radius is hot enough to make UV radiation and the resultant effect of photo-ionization line-driving at the outer light cylinder bends the upward flowing plasma outward over the accretion disk and generates a bi-conic Elvis outflow structure of positive ions associated with the broad emission line region (BELR). In this latter context the process of charge separation between the electrons and out-flowing positive ions is generated by the effects of photo-ionization occurring near the MECO light cylinder. The return current of negative electrons most likely flows back to the central region along the separatrix associated with magnetic field-line opening due to the differential rotation which occurs in the magnetically linked MECO disk system.

Hence in the context of the MECO-quasar model the existence of a bi-conic elliptical coronal outflow structure, like that shown in figure 1 of Elvis astro-ph\0311436v1), but which now has a characteristic radius located just inside of the outer light cylinder of central MECO surrounded by a hot magneto-spherically truncated accretion disk, is an intrinsically predicted observational property of the MECO-quasar accretion disk model that uniquely distinguishes it from a black hole–quasar accretion disk model.

In contrast to the case of a rotating Black Hole, surrounded by a accretion disk containing a magnetic field which threads its event horizon, the intrinsic dipolar magnetic field lines of a MECO are physically anchored to the highly red-shifted rotating time-like surface of the MECO. In addition, region outside of the Eddington limited timelike MECO surface, which is described by a highly red-shifted, rotating Vaidya metric, can be well approximated to first order by a rotating Kerr metric. Hence in this first order approximation we can use the Kerr metric formula (Rufini, R., Christodoulu, D., Phys. Rev, D, Vol 4 3552, 1971)

$$(M\nu_S) / [(2 \times 10^5 \text{ Hz})] = \{(a/M) / [\{1+ (1-(a/M)^2)^{1/2}\}^2 + (a/M)^2]\} \quad (1)$$

in order to determine the spin frequency ν_S seen by a distant observer, of the intrinsic, equipartition, dipolar magnetic field lines anchored to the highly red-shifted rotating MECO surface. In equation (1) (a/M) is the specific angular momentum ratio of the MECO, ν_S is the MECO surface spin in Hz = cycles/sec, and M is the MECO mass in units of solar masses Mo.

Now because of large magnetic braking effects associated with the existence of the very strong intrinsic magnetic field anchored to its highly red shifted surface, the central MECO inside of a quasar will always tend to be a very slow rotator with (a/M) << 1. This is reflected in the calculations shown in table 2, 3, 4, and 5 where it can be seen that quantity $(M\nu_S)$ ranges over 10 to 100. Hence the quantity on the left hand side of equation (1) given by $(M\nu_S) / [(2 \times 10^5 \text{ Hz}]$ is very small and ranges over 10^{-5} to 10^{-4}. Since the quantity (a/M) on the right hand side of equation (1) is restricted to range over 0 to 1 this implies that equation (1) can be solved only in an approximation where (a/M) <<< 1 as

$$\mathbf{(a}/M) = \mathbf{[}(2 \times 10^{-5}\mathbf{)]}\ (M\nu_S) \quad << 1 \quad (2)$$

Now in the context of the above described model for MECO-Quasars we argued earlier that the broad line region associated with the radius Rblr is generated by the effects of UV line driving that occur near the MECO outer light cylinder located at Rlc. We can formally expressed this property of the MECO-quasar model as

$$Rblr = \lambda\ Rlc \quad (3)$$

where $\lambda \leq 1$, Rlc is the MECO outer light cylinder in units of $Rg = GM/c^2$ given by

$$Rlc = (3.2 \times 10^4 Rg) / (M\nu) \quad (4)$$

Hence from equations (2), (3), and (4) we see that in the MECO-Quasar model a linear relationship exists between the MECO-Quasar's specific angular momentum ratio (a/M) and the ratio (Rg/ Rblr), associated with the inverse of the radius of the broad line region generated by the bi-conic Elvis structure above and below the accretion disk surrounding the MECO, given by

$$(\mathbf{a}/M) = (0.64\lambda \ (Rg / Rblr) \quad (5)$$

where $Rg = GM/c^2$, and $\lambda \leq 1$. In order to use equation (5) to calculate the value of the specific angular momentum ratio (a/M) for a MECO-Quasar both the mass M of its central MECO and the characteristic radius Rblr of its broad line region need to be observationally determined, and for large numbers of quasars it can be difficult to obtain the needed observational data.

However there is a more efficient way of using equation (5) to determine the value of (a/M) for MECO-Quasars if as input we use the observationally determined empirical correlation between the size of the broad line region Rblr of a Quasar and its bolometric Eddington ratio (Lbol / LEdd) given by the empirical formula (Kaspi, et. al. 2005)

$$Rblr = [(2.79 \pm 0.14) \times 10^4 Rg)] (M_8)^{(-0.35) \pm (-0.04)} (Lbol/LEdd)^{(0.65) \pm (0.04)} \quad (6)$$

In order to test the compatibility of the Kaspi et. al correlation equation (6) with the size of the broad line regions predicted by the MECO model for quasars described by equations (1) thru (5), a new set of calculations which now included equations (1) thru (6) were performed for the two MECO-Quasars Q2237 and Q0957. The results of these new calculations are shown in Table 1 and Table 2 in Appendix I where it is shown that the new MECO model for quasars Q2237 and Q0957 respectively satisfy the Kaspi correlation equation (6) as

$$Rblr = [(2.93 , 2.79) \times 10^4 Rg)] (M_8)^{(-0.31)} (Lbol/LEdd)^{(0.69)} \quad (6\text{-a})$$

a result which is clearly within the error bars of equation (6). Nonetheless consistently incorporating equations (1) thru (6) into the new MECO models for Q0957 and Q2237 has the effect of causing them to have slightly different masses (4.1×10^9 Mo and 4.2×10^9 Mo respectively) than the earlier models, and the values of their specific angular momentum ratios (a/M) are now predicted to have the very small values of 0.002 and 0.0005 respectively. In tables 3, 4, and 5 in Appendix I, the results similar calculations performed for a large database of radio loud and radio quiet quasars are also given.

Having verified that the Kaspi correlation equation (6) is compatible with the MECO-Quasar model, we next note that equation (5) can be simply interpreted as implying that the specific angular momentum ratio (a/M) of a MECO-quasar represents a linear proxy for the ratio (Rg / Rblr), associated with the reciprocal of the radius of its broad line region. Hence, because of the linear proxy relationship between (a/M) and (Rg/Rblr) represented by the MECO equation (5), this implies that we are justified in using the MECO model equation (5) with the empirical Kaspi correlation formula (6) in order to formally obtain a empirical relationship that correlates the MECO specific angular momentum ratio (a/M) to the MECO mass $M = (M / 10^8 Mo)$ and the bolometric Eddington ratio (Lbol / LEdd) as

$$(a/M) = (2 \times 10^{-5}) (3.2\lambda / 2.79) (M_8)^{(0.35)} (Lbol/LEdd)^{-(0.65)} \qquad (7)$$

Recalling that the MECO model for quasars requires that $\lambda \leq 1$, then to a good approximation we expect that $(3.2\lambda / 2.79) \sim 1$. In this context the empirical correlation between MECO specific angular momentum ratio (a/M), the MECO mass $M_8 = (M / 10^8 Mo)$, and bolometric Eddington ratio (Lbol / LEdd), is

$$(a/M) \sim (2 \times 10^{-5}) (M_8)^{(0.35)} (Lbol/LEdd)^{-(0.65)} \qquad (8)$$

In summary we see that by combining the MECO model described in equations (1) thru (5) with the observationally determined empirical Kaspi correlation relationship between the size of the broad line region Rblr of a Quasar and its bolometric Eddington ratio (Lbol / LEdd) represented by equation (6), we are led to equation (8) which defines the MECO-QUASAR FUNDAMENTAL PLANE (MQFP).

The MQFP determines the specific angular momentum (a/M) of a MECO-Quasar in terms of two observational proxies, the quasar mass $M_8 = (M / 10^8 Mo)$, and

the quasar Eddington ratio (Lbol / LEdd). Since Quasar masses and Eddington ratios range over ($10^{-1} < M_8 < 10^2$) and (0.001< (Lbol/LEdd) < 1) respectively, we see that the MQFP equation (8) predicts that MECO-Quasars have values of (a/M) << 1 consistent with the assumptions under which it was derived.

As discussed in Appendix I, MECO-Quasars with (a/M) <<1 dynamically operate within the context of three fundamental spectral states which are controlled the values of their bolometric Eddington ratios Lbol/LEdd:

(1) The Radio Loud Low Hard State (RL-LHS), (0.0001 < Lbol/LEdd < 0.02), where the magnetospheric radius of the MECO accretion disk lies outside of the MECO co-rotation radius (Rm > Rc).
(2) The Radio Quiet High Soft State (RQ-HSS), (0.02 < Lbol/LEdd < 0.1), where the magnetospheric radius of the MECO accretion disk lies within (3Rg < Rm < 6Rg)
(3) The Radio Loud Very High State (RL-VHS), (0.1 < Lbol / LEdd < 1), where the magnetospheric radius of the MECO accretion disk lies just outside of the MECO surface (Rm > 2 Rg)

Note that because of the large magnetic braking effects associated with the existence of the very strong intrinsic magnetic field anchored to its highly red shifted surface, the central MECO inside of a quasar will always tend to be a very slow rotator with (a/M) << 1. This result contrasts with the case of Black Hole models for quasars, where large values of (a/M) ≤ 1 are required since the magnetic fields reside only in their accretion disks. However even though (a/M) << 1 for MECO-quasar models in High States, MECO-quasar models remain observationally viable with respect to the observation of broad Iron line emission in High States because Fe Iron lines can be generated in their accretion disks outside of the photon sphere in a radial zone (3Rg ≤ Rm < 6Rg) consistent with observations. For example as shown in Table 2 for the case of Q2237 in the RQ-HSS with M=4.1 x 10^9 Mo and (a/M) = 0.0005, a broad Fe-alpha Iron line is formed at the radius Rm = 3.1 Rg (Schild, Leiter, and Robertson, Astron. Journ.,v135, p947, (2008)). This occurs because the inner magnetospheric radius Rm of the accretion disk of a MECO-Quasar in a High State becomes dynamically balanced against the effects of gravity outside of the photon sphere by strong magnetic pressure forces generated by the MECO's intrinsic magnetic field.

In addition we also note that it has been recently suggested (Nowak, M.A., Juett, A., Homan, J., Yao, Y., Wilms, J., Schulz, N.S., Canizares, C.R.ApJ, 689, 1199, (2008)) that the observable effects of the high soft states, associated with an AGN which contains a slowly rotating ($a/M << 1$) black hole surrounded by an accretion disk with a hot corona (perhaps which is magnetically heated Laor & Behar arXiV:0808.0637v1 (2008)), can quantitatively mimic the observable effects of high soft states associated with an AGN which contains a rapidly rotating ($a/M \sim 1$) black hole surrounded by an accretion disk without a hot corona. In this context the $a/M << 1$ result associated with MECO-quasars is can be shown to be observationally viable since the strong intrinsic magnetic fields of the central MECO in quasars would automatically generate a hot magnetically heated corona surrounding the inner region of their accretion disks.

In terms of the three spectral states of a MECO-Quasar, equation (8) representing the MQFP is graphically plotted in figure 1 with the calculated data points contained in Tables 3, 4, and 5 as given in Appendix I. As shown in figure 1 the result of this plot implies that quasars in the higher luminosity RQ-HSS and RL-VHS states are correlated with lower values of the specific angular momentum ratio (a/M) of their central MECO, while quasars in the lower luminosity RL-LHS states are correlated with higher values of the specific angular momentum ratio (a/M) of their central MECO. Hence in the context of the three fundamental MECO-Quasar states discussed in Appendix I, the picture presented by MQFP describes a cosmological scenario where: younger, higher luminosity QSO observed in their RQ-HSS and RL-VHS states are in the process of spinning up their central MECO from initially lower values of (a/M); while older, lower luminosity QSO observed in their RL-LHS states are in the process of spinning down their central MECO from initially higher values of (a/M).

Hence this implies a cosmological scenario where black holes are initially born with low levels of rotation, and are rapidly sped up in an early chaotic universe at higher mean density and less systematic rotation. In the more local universe, galaxy interactions are presumably less frequent and quasar fueling less important, causing mean quasar rotation to slow due to the angular momentum losses resulting from rotation-powered radiation.

If this is the case then evidence for this type of evolution of quasar states over cosmological time could be sought in radio observations of high red shift quasars. For example it is well known that evolution in quasar properties is observed in the local universe, with few quasars found below $z = 0.3$. On the other hand in the red

shift range z = 1 - 3, most quasars are radio quiet and therefore could be interpreted as being MECO-quasars in the Radio Quiet High Soft State.

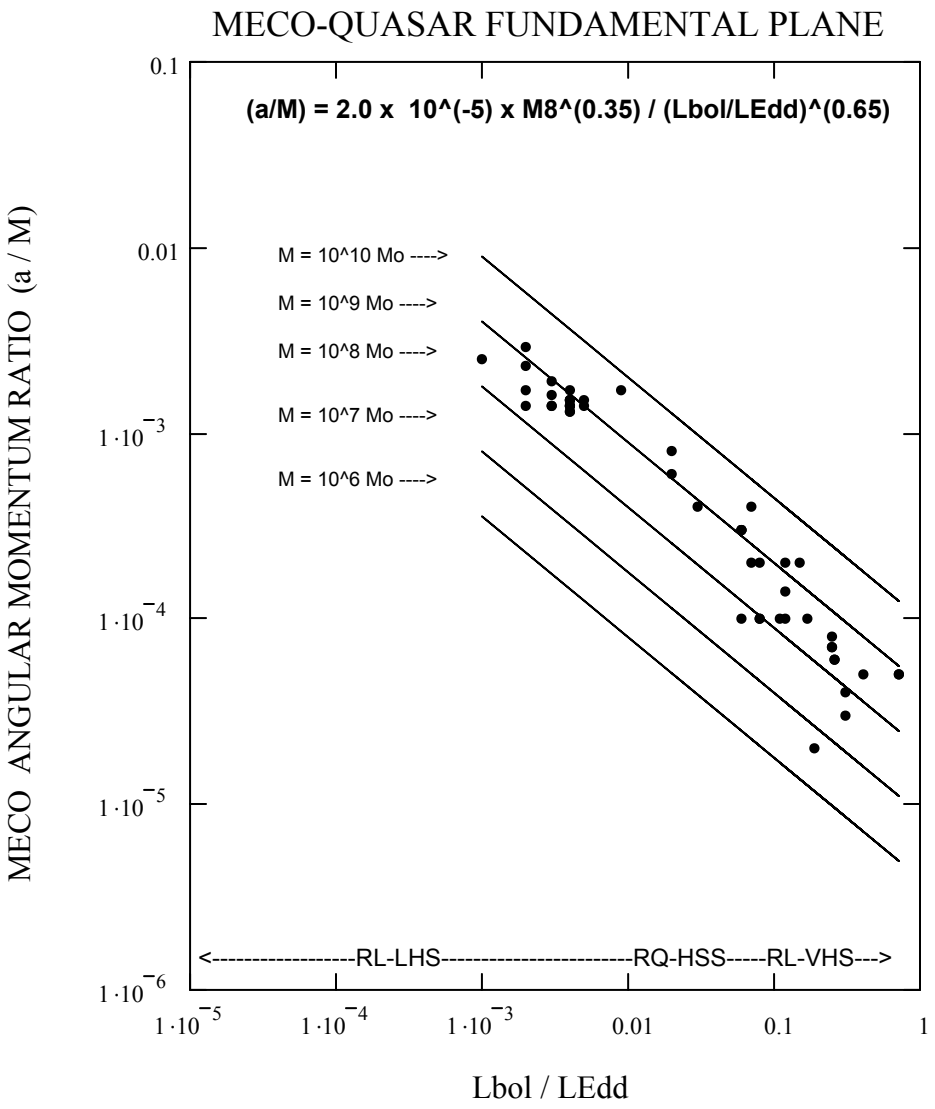

We plot the MECO-QUASAR FUNDAMENTAL PLANE as a function of log(a/M) versus log(Lbol / LEdd). We do this over the three ranges:

0.1 < Lbol/LEdd < 1.0 RADIO LOUD VERY HIGH STATE
0.02 < Lbol/LEdd < 0.1 RADIO QUIET HIGH SOFT STATE
0.001 < Lbol/LEdd < 0.02 RADIO LOUD LOW HARD STATE

for four values of the MECO mass ranging from 10^6 Mo to 10^10 Mo. We then add in observed data points taken from the literature. The data is associated with:

a) low redshift "quasar-like" radio galaxies in the low hard state (which in the MECO theory are now identified as being a "low redshift, low luminosity" component of the quasar population)
b) high redshift radio loud quasars in the low hard state
c) high redshift radio quiet quasars in the high soft state
d) high redshift radio loud quasars in the very high state

We see that that all of these quasars lie within the predicted regions

APPENDIX I. THE THREE FUNDAMENTAL STATES OF A MECO-QUASAR

1) THE RADIO LOUD LOW HARD STATE (RL-LHS) OF A MECO-QUASAR

The Radio Loud Low Hard State (RL-LHS) of a MECO-quasar which occurs in the Eddington ratio range (0.0001 < Lbol / LEdd < 0.02) has been discussed in detail for the case of the quasar Q0957 (Schild, Leiter, & Robertson, 2006) Under these conditions the magnetospheric radius of the MECO accretion disk lies outside of the MECO co-rotation radius (Rm > Rc). Because the magnetospheric radius of the accretion in the RL-LHS is outside of the co-rotation radius, the intrinsically dipole magnetic field lines of the MECO are rotating more rapidly than the accretion disk. This allows the MECO magnetic propeller to operate efficiently which creates a unique internal magnetospheric accretion disk structure for the quasar and a strong jet structure associated with radio loud emissions. In this context angular momentum is transferred from the MECO to the accretion disk by the magnetic propeller and causes a spin-down of the MECO specific angular momentum ratio (a/M) to occur.

2) THE RADIO QUIET HIGH SOFT STATE (RQ-HSS) OF A MECO-QUASAR

The Radio Quiet High Soft State (RQ-HSS) of a MECO-quasar occurs in the Eddington ratio range (0.02 < Lbol / LEdd < 0.1) has been discussed in detail for the case of the quasar Q2237 (Schild, Leiter, & Robertson, 2008). In general for a MECO-quasar running at this higher Eddington ratio range the magneto-spheric radius Rm of its accretion disk will be pushed inside of the MECO co-rotation radius Rc. This causes radio emitting jet to die out since the MECO magnetic propeller that was generating it is shut down when Rm < Rc occurs. For these higher accretion rates the intrinsic magnetic propeller mechanism of the MECO is incapable of stopping the flow and a boundary layer forms at the inner disk radius.

The existence of such a boundary layer in the radio quiet high soft state (RQ-HSS) associated with these higher accretion rates can be seen by comparing the magnetic pressure at the magnetosphere with the impact pressure of its trailing, subsonic disk. This is because at higher accretion rates associated with the Radio Quiet High Soft State (RQ-HSS) it has been found that unphysical radial inflow disk velocities in excess of the speed of light would be required to allow the impact pressure match the magnetic pressure.

Under these conditions the MECO magnetic field cannot eject the disk material from the radial region inside of the co-rotation radius Rc and the matter accreted by the gravitational force piles up against the magnetopause and pushes the radius of the magnetosphere further inward. This causes the the MECO magnetospheric radius Rm to fall into a zone where it becomes dynamically balanced again within (3Rg < Rm < 6Rg) due to the effects of three forces:

1) the strong outward magnetic pressure force generated at the magnetospheric radius Rm by the central MECO magnetic field ~ 10^6 G,
2) the outward centrifugal force exerted on the accretion disk at Rm and,
3) the inward gravitational force acting on the accreted matter piled up against the magnetosphere.

In the equilibrium state associated with the RQ-HSS, the state of the disk from the magnetospheric Rm outwards remains gas pressure dominated. This is because in this process gas pressure in the disk necessarily matches up with the magnetic pressure, and radiation pressure in the disk remains well below gas pressure.

Since the magnetospheric radius Rm of the accretion lies inside of the co-rotation radius Rc in the RQ-HSS, the intrinsic dipole magnetic field lines of the MECO are rotating more slowly than the Keplarian rotation of the accretion disk at Rm. In this context angular momentum is transferred from the accretion disk to the MECO via the interaction of its intrinsic dipole field lines with the disk which causes a spin-up of the MECO specific angular momentum ratio (a/M) to occur. Nonetheless, since the MECO magnetic propeller cannot operate efficiently, there is no jet structure created in the (RQ-HSS) and this state of the MECO-Quasar is radio quiet.

In the following Tables we apply the MECO model equations given in Table 1 to the case of Q2237 in the (RQ-HSS) and Q0957 in the (RL-LHS) as shown in Table 2. We then do similar calculations in Tables 3 and 4 for a larger database of Quasars in the (RQ-HSS) and (RL-LHS) respectively

Table 1: MECO-QUASAR MAGNETOSPHERIC EQUATIONS FOR RL-LHS, RQ-HSS, AND RL-VHS - [ref. Astr J. v132,420,(2006) and Astr J. v135,947 (2008) and Appendix I]

MECO Physical Quantity	Equation	Scale
Surface Redshift -	$1 + z_s = 1.5 \times 10^8 (M/7)^{1/2}$	$M^{1/2}$
Surface Luminosity -	$L_s = L_{Edd}/(1 + z_s)$ erg/s	$M^{1/2}$
Surface Temp. -	$T_s = 2.3 \times 10^7/[M(1 + z_s)]^{1/4}$ K	$M^{-3/8}$
Magnetic Moment -	$\mu_{27} = 8.16[L_{c,36} M/\nu_2^3]^{1/2}$ cm	$M^{5/2}$
Magnetic Field -	$B_\theta = 1.12(R_g/r)^3 [L_{c,36}/(M^5 \nu_2^3)]^{1/2}$ gauss	$M^{-1/2}$
Quiescent Lum. -	$L_{q,32} = 0.65M[L_{c,36}/M]^{1.75}$ erg/s	M
Rotation Rate -	$\nu_2 = 0.89[L_{q,32}/M]^{0.763}/L_{c,36}$ Hz	M^{-1}
a/M Ratio -	$a/M = 2.0 \times 10^{-3}(M\nu_2)$	M^0
Core X-ray Luminosity -	$L_x = \eta_{x-corona} L_{disk}$ erg/s	M
Light Cylinder Radius -	$R_{lc} = 320 R_g/[M\nu_2]$ cm	M
Co-rotation Radius -	$R_c = 46.7 R_g/[M\nu_2]^{2/3}$ cm	M
Magnetosphere Radius (RL-LHS) -	$R_m = 17 R_g [M\nu_2]^{4/21}/(L_{disk-jet}/L_{Edd})^{2/7}$ cm	M
Kinetic Power into Jet (RL-LHS) -	$W_{jet,36} = C_{disk-jet} L_{disk,36}^{2/3} \lvert 1 - (L_{disk,36}/L_{c,36})^{1/3} \rvert$ erg/s	$M^{2/3}$
Core Radio Luminosity (RL-LHS) -	$L_{rad,36} = C_{rad-x} M^{0.8} L_{x,36}^{2/3} \lvert 1 - (L_{x,36}/L_{c,36})^{1/3} \rvert$ erg/s	$M^{3/2}$
Magnetosphere Radius (RQ-HSS) -	$(3R_g < R_m < R_c)$ cm	M
Magnetosphere Radius (RL-VHS) -	$(2R_g < R_m)$ cm	M
Kinetic Power into Jet (RL-VHS) -	$W_{jet,36} = 350M$ erg/s	M
Core Radio Luminosity (RL-VHS) -	$L_{rad,36} = C_{rad-jet} W_{jet,36}$ erg/s	M

Table 2: TWO MECO-QUASAR STATES: Q2237(RQ-HSS) - Q0957(RL-LHS)

MECO Parameters	QUASAR 2237 (RQ-HSS)	QUASAR Q0957 (RL-LHS)
MECO Mass	$4.1 \times 10^9 M_\odot$	$4.2 \times 10^9 M_\odot$
MECO Magnetic Moment	1.7×10^{52} gauss-cm^3	1.8×10^{52} gauss-cm^3
MECO a/M Ratio	0.0005	0.002
MECO Surface Redshift	3.6×10^{12}	3.7×10^{12}
MECO Rotation Period	5.6 Years	1.6 Years
MECO Surface Luminosity	1.5×10^{35} erg/sec	1.5×10^{35} erg/sec
MECO Surface Temp	66 K	66 K
Accretion Disk Luminosity	3.2×10^{46} erg/sec	4.6×10^{45} erg/sec
Eddington Ratio	6.0×10^{-2}	9.0×10^{-3}
Kinetic Power into Jet-Corona	1.0×10^{41} erg/sec	1.0×10^{45} erg/sec
Disk Corona Jet Power Coefficent	$C_{disk-jet} = 2.0 \times 10^{-3}$	$C_{disk-jet} = 1.8 \times 10^3$
Core X-ray Luminosity	1.6×10^{44} erg/sec	2.5×10^{45} erg/sec
Core Radio Luminosity	1.0×10^{40} erg/sec	3.7×10^{42} erg/sec
Core X-ray Efficiency	$\eta_{x-corona} = 0.003$	$\eta_{x-corona} = 0.54$
Core Radio X-ray Luminosity Coefficient	$C_{rad-x} = 6.6 \times 10^{-9}$	$C_{rad-x} = 3.5 \times 10^{-7}$
Co-rotation Radius Rc - cm	$R_c = 123 R_g = 7.6 \times 10^{16}$	$R_{(c)} = 53 R_g = 3.4 \times 10^{16}$
Magnetospheric Radius Rm - cm	$R_m = 3.1 R_g = 1.9 \times 10^{15}$	$R_m = 64 R_g = 4 \times 10^{16}$
MECO Magnetic Field at Rm	$(3.4 \times 10^5$ gauss$)(R_m/r)^3$	(35 gauss$)(R_m/r)^3$
Thickness of Hot Inner Ring - cm	$\delta(R) = 0.04 R_g = 3.0 \times 10^{13}$	$\delta(R) = 0.9 R_g = 5.4 \times 10^{14}$
Wein Peak of Hot Inner Ring	$450 A_o$	$4374 A_o$
Light Cylinder - cm	$R_{lc} = 8.4 \times 10^{17}$	$R_{lc} = 2.4 \times 10^{17}$
BLR Elvis Structure - cm	$R = 8.2 \times 10^{17}$ $H = 1.6 \times 10^{17}$	$R = 2 \times 10^{17}$ $H = 5 \times 10^{16}$
Base of Radio Jet - cm	RADIO QUIET-NO JET	$R = 2 \times 10^{16}$ $H = 9 \times 10^{16}$
Kaspi Correlation - 0.69 Power Law	$Norm - Coeff = 2.93$	$Norm - Coeff = 2.79$

Table 3

QUASARS AND "QUASAR-LIKE" RADIO GALAXIES IN MECO RADIO LOUD (RL-LHS)

	Lbol	Lrad	M/Mo	Lbol / LEdd	a/M	μ(G-cm^3)	T(days)	Rblr(cm)	Rm(cm) > Rc(cm)	
Q0957+561	$10^{45.7}$	$10^{42.6}$	$10^{9.6}$	0.009	0.0017	$10^{52.3}$	577	$10^{17.4}$	$10^{16.6}$	$10^{16.5}$
Q0317+183	$10^{45.0}$	$10^{41.8}$	$10^{9.2}$	0.004	0.0020	$10^{52.1}$	183	$10^{16.8}$	$10^{16.3}$	$10^{16.0}$
Q0537-441	$10^{46.0}$	$10^{44.0}$	$10^{9.9}$	0.010	0.0018	$10^{53.0}$	1022	$10^{17.6}$	$10^{16.9}$	$10^{16.8}$
FR1 0316+41	$10^{44.9}$	$10^{42.2}$	$10^{9.1}$	0.005	0.0015	$10^{51.0}$	192	$10^{16.9}$	$10^{16.1}$	$10^{16.0}$
FR2 0131-36	$10^{44.8}$	$10^{40.9}$	$10^{9.0}$	0.005	0.0014	$10^{50.7}$	162	$10^{16.8}$	$10^{16.0}$	$10^{15.9}$
FR2 1350+31	$10^{44.4}$	$10^{40.6}$	$10^{8.7}$	0.004	0.0014	$10^{50.0}$	85	$10^{16.5}$	$10^{15.8}$	$10^{15.7}$
FR1 0325+024	$10^{44.3}$	$10^{40.5}$	$10^{8.6}$	0.004	0.0013	$10^{49.7}$	72	$10^{16.5}$	$10^{15.7}$	$10^{15.6}$
FR2-0936+07	$10^{44.5}$	$10^{40.4}$	$10^{8.8}$	0.004	0.0015	$10^{50.2}$	100	$10^{16.6}$	$10^{15.9}$	$10^{15.7}$
FR1 2236-176	$10^{44.5}$	$10^{41.6}$	$10^{8.8}$	0.004	0.0015	$10^{50.2}$	100	$10^{16.6}$	$10^{15.9}$	$10^{15.7}$
FR1 2322-122	$10^{44.4}$	$10^{40.0}$	$10^{8.8}$	0.004	0.0017	$10^{50.2}$	85	$10^{16.5}$	$10^{15.9}$	$10^{15.7}$
FR1 0305+03	$10^{44.6}$	$10^{41.2}$	$10^{8.8}$	0.004	0.0013	$10^{50.2}$	117	$10^{16.7}$	$10^{15.8}$	$10^{15.7}$
FR2 1448+63	$10^{44.4}$	$10^{39.7}$	$10^{8.7}$	0.004	0.0014	$10^{50.0}$	85	$10^{16.5}$	$10^{15.8}$	$10^{15.7}$
FR2 0123-01	$10^{44.4}$	$10^{40.6}$	$10^{8.7}$	0.004	0.0014	$10^{50.0}$	83	$10^{16.5}$	$10^{15.8}$	$10^{15.6}$
FR1 1626+39	$10^{44.5}$	$10^{40.3}$	$10^{8.8}$	0.004	0.0015	$10^{50.2}$	91	$10^{16.6}$	$10^{15.9}$	$10^{15.7}$
FR1 0055-01	$10^{44.4}$	$10^{40.3}$	$10^{8.9}$	0.003	0.0019	$10^{50.3}$	84	$10^{16.5}$	$10^{16.0}$	$10^{15.7}$
FR2 0634-206	$10^{44.3}$	$10^{40.0}$	$10^{8.7}$	0.003	0.0016	$10^{50.0}$	72	$10^{16.5}$	$10^{15.8}$	$10^{15.6}$
FR1 0915-118	$10^{44.7}$	$10^{40.3}$	$10^{8.9}$	0.003	0.0014	$10^{50.5}$	138	$10^{16.8}$	$10^{16.0}$	$10^{15.9}$
FR2 0106-02	$10^{44.0}$	$10^{40.3}$	$10^{8.5}$	0.003	0.0014	$10^{49.5}$	50	$10^{16.3}$	$10^{15.6}$	$10^{15.4}$
FR1 0331-01	$10^{44.8}$	$10^{41.2}$	$10^{9.0}$	0.002	0.0014	$10^{50.7}$	161	$10^{16.8}$	$10^{16.0}$	$10^{15.9}$
FR2 1842+30	$10^{44.6}$	$10^{41.1}$	$10^{9.2}$	0.002	0.0029	$10^{51.2}$	121	$10^{16.7}$	$10^{16.4}$	$10^{15.9}$
FR1 1610+296	$10^{44.5}$	$10^{39.1}$	$10^{9.0}$	0.002	0.0023	$10^{50.6}$	91	$10^{16.6}$	$10^{16.1}$	$10^{15.7}$
FR1 1333-331	$10^{43.9}$	$10^{41.2}$	$10^{8.5}$	0.002	0.0017	$10^{49.5}$	42	$10^{16.2}$	$10^{15.7}$	$10^{15.4}$
FR2 0356+10	$10^{43.7}$	$10^{39.3}$	$10^{8.5}$	0.001	0.0025	$10^{49.5}$	30	$10^{16.0}$	$10^{15.8}$	$10^{15.3}$

Table 4

QUASARS IN MECO RADIO QUIET HIGH SOFT SPECTRAL STATES IN RADIO QUIET (RQ-HSS)

	Lbol	M / Mo	Lbol / Ledd	a/M	T(years)	μ(G-cm^3)	Rblr(cm)	Rcont(cm)	Rline(cm)
Q2237+0305	$10^{46.4}$	$10^{9.5}$	0.06	0.0003	5.6	$10^{51.9}$	$10^{17.9}$	$10^{15.7}$	$10^{15.3}$
WFIJ2033-4723	$10^{45.8}$	$10^{8.8}$	0.08	0.0002	2.3	$10^{50.2}$	$10^{17.5}$	$10^{15.0}$	$10^{14.6}$
HE0230-2130	$10^{45.5}$	$10^{6.5}$	0.08	0.0001	1.4	$10^{49.5}$	$10^{17.3}$	$10^{14.7}$	$10^{14.3}$
RXJ1131-1231	$10^{44.9}$	$10^{7.9}$	0.08	0.0001	0.5	$10^{48.0}$	$10^{16.9}$	$10^{14.1}$	$10^{13.7}$
H1413+117	$10^{46.8}$	$10^{9.8}$	0.07	0.0004	11.3	$10^{52.8}$	$10^{18.2}$	$10^{16.0}$	$10^{15.6}$
RXJ0911+0551	$10^{46.1}$	$10^{9.2}$	0.06	0.0003	3.5	$10^{51.2}$	$10^{17.7}$	$10^{15.3}$	$10^{15.0}$
PG1115+080	$10^{46.0}$	$10^{9.1}$	0.06	0.0003	3.0	$10^{51.0}$	$10^{17.7}$	$10^{15.3}$	$10^{14.6}$
SDSSJ0924+0219	$10^{44.8}$	$10^{7.9}$	0.06	0.0001	0.4	$10^{48.0}$	$10^{16.8}$	$10^{14.1}$	$10^{13.7}$
0054-144	$10^{45.5}$	$10^{8.9}$	0.03	0.0004	1.3	$10^{50.5}$	$10^{17.3}$	$10^{15.1}$	$10^{14.7}$
1029-140	$10^{46.0}$	$10^{9.1}$	0.07	0.0002	3.2	$10^{50.9}$	$10^{17.7}$	$10^{15.3}$	$10^{14.9}$
0157+001	$10^{45.6}$	$10^{9.0}$	0.03	0.0004	1.7	$10^{50.7}$	$10^{17.4}$	$10^{15.2}$	$10^{14.8}$
0204+292	$10^{45.1}$	$10^{8.5}$	0.03	0.0003	0.7	$10^{49.5}$	$10^{17.0}$	$10^{14.7}$	$10^{14.3}$
0205+024	$10^{45.5}$	$10^{8.7}$	0.04	0.0003	1.3	$10^{50.0}$	$10^{17.3}$	$10^{14.9}$	$10^{14.5}$
0244+194	$10^{45.5}$	$10^{9.1}$	0.02	0.0006	1.4	$10^{51.0}$	$10^{17.3}$	$10^{15.3}$	$10^{14.9}$
0923+201	$10^{46.2}$	$10^{9.6}$	0.03	0.0006	4.4	$10^{52.2}$	$10^{17.8}$	$10^{15.8}$	$10^{15.4}$
1012+008	$10^{45.5}$	$10^{9.1}$	0.02	0.0006	1.4	$10^{51.0}$	$10^{17.3}$	$10^{15.3}$	$10^{14.9}$
1116+215	$10^{46.0}$	$10^{9.6}$	0.02	0.0008	3.1	$10^{52.2}$	$10^{17.7}$	$10^{15.8}$	$10^{15.4}$

3) THE RADIO LOUD VERY HIGH STATE (RL-VHS) OF A MECO-QUASAR

As long as it operates in the Eddington ratio regime ($0.02 < Lbol / LEdd < 0.1$) associated with the (RQ-HSS), the above described dynamic equilibrium for the magnetospheric radius occurring in the radial zone ($3Rg < Rm < 6Rg$) outside of the Photon Sphere can be maintained.

However for MECO-Quasars running in the higher accretion Eddington ratios ($0.1 < Lbol / LEdd < 1$), the magnetospheric radius Rm of the MECO accretion disk is eventually pushed inside of the radius of the MECO photon sphere at 3Rg. This dynamically acts like a spectral switch because inside of 3Rg the centrifugal force component acting on the magnetospheric radius Rm becomes reversed in sign (Abramowicz, SCI-AM, March 1963). Because of the centrifugal force reversal which occurs inside of 3Rg, the dynamical balance associated with the (RQ-HSS) cannot be maintained and the magnetospheric radius Rm falls down into the radial zone just outside of the MECO surface at $Rm \geq 2Rg$. There it becomes dynamically stabilized just outside of 2Rg by the repulsive action of the very strong outward magnetic pressure forces associated with the ~ 10^20 G magnetic fields which emanate from the timelike Eddington limited surface of the MECO. Under these conditions Chou-Tajima plasma dynamo mechanism (Chou, Tajima (1999) becomes efficient and generates a powerful radio jet associated with the MECO-quasar Radio Loud Very High State (RL-VHS).

The Chou-Tajima plasma dynamo mechanism operates when a strong enough outward pressure source exists just outside of 2Rg that provides the balancing force to stop the radial infall of the plasma. In the case of the MECO-quasar the pressure source is automatically supplied by the repulsive action of the very strong outward magnetic pressure forces associated with the ~ 10^20 G magnetic fields which emanate from the Eddington limited timelike surface of the MECO. Under these conditions, when a toroidal field exists, the plasma near the surface of the MECO can become subject to “magnetic buoyancy instabilities”. This instability will be largely suppressed, however, if a poloidal magnetic field exists in the region.

Since the MECO is slowly rotating $(a/M) << 1$ the inner edge of its accretion disk at the magnetospheric radius $Rm \geq 2Rg$ will lie well inside of the co-rotation radius of the MECO. Hence the inner edge of the accretion disk will be rotating much faster than the rotation rate of the intrinsic magnetic dipole field lines emanating form the surface of the MECO.

This will cause the the MECO poloidal magnetic field penetrating the plasma of the rotating accretion disk to become twisted and changed into a toroidal field, which will cause the plasma in the disk to become episodically destabilized due to the magnetic buoyancy instability. The manifestation of this episodic instability will create a jet formation emanating from the inner region of the MECO accretion disk atmosphere. Since this formation mechanism is deep in the gravitational potential of the MECO, the energy liberated and the jet formed by this mechanism will be very substantial.

Under these conditions the electromagnetic power output into the jet, as seen by a distant observer, from the inner region of the accretion disk of a MECO quasar in the RL-VHS, which is generated by a MECO version of the Chou-Tajima mechanism can be estimated from (Chou, Tajima (1999), and section 2.2 of (Livio, Ogilvie, & Pringle, 1998), to be given by

$$Wjet \sim Cjet\,[(Bpolodial\text{^}2)/4\pi]\,(\pi\, Rd\text{^}2)\,(Rd\Omega)$$

where for the MECO-Quasar we find that

$$Bpoloidal \sim (10\text{^}20G) / [(1+ z_S)/20]$$

$$(1+z_S) \sim (1.5 \times 10\text{^}8)\,(M / 7)\text{^}(1/2)$$

$$(Rd\Omega) \sim 1$$

$$Rd \sim (3 \times 10\text{^}5) \times M / 20 = 1.5 \times M \times 10\text{^}4$$

and $Cjet \sim 3.7 \times 10\text{^}4$

Hence this implies that in the RL-VHS, Wjet scales with the mass of the MECO as

$$Wjet \sim (3.51 \times 10\text{^}38)\, M \quad erg/sec$$

In the following Table 5 we apply the above MECO model equations in addition to those given in Table 1 to a large database of Quasars in the (RL-VHS)

Table 5

QUASARS IN MECO RADIO LOUD VERY HIGH STATES (RL-VHS)

	Lbol	Lrad	M / Mo	Lbol / Led	a/M	μ(G-cm^3)	T(years)	Rblr(cm)	Rcont(cm)	Rline(cm)
FRSQ 1633+382	$10^{46.5}$	$10^{44.4}$	$10^{9.2}$	0.17	0.0001	$10^{51.2}$	7.1	$10^{18.0}$	$10^{15.4}$	$10^{14.9}$
FSRQ 0420-014	$10^{47.0}$	$10^{43.5}$	$10^{9.0}$	0.72	0.00005	$10^{50.8}$	15.1	$10^{18.4}$	$10^{15.2}$	$10^{14.7}$
FSRQ 2230+114	$10^{46.2}$	$10^{44.2}$	$10^{9.0}$	0.12	0.0002	$10^{50.7}$	4.3	$10^{17.8}$	$10^{15.2}$	$10^{14.7}$
FSRQ 2223-032	$10^{45.1}$	$10^{43.9}$	$10^{7.9}$	0.11	0.0001	$10^{48.0}$	0.7	$10^{17.0}$	$10^{14.1}$	$10^{13.6}$
FSRQ 1253-055	$10^{46.1}$	$10^{43.8}$	$10^{8.9}$	0.12	0.00014	$10^{50.5}$	3.6	$10^{17.7}$	$10^{15.1}$	$10^{14.6}$
FSRQ 0736+017	$10^{46.0}$	$10^{42.2}$	$10^{8.5}$	0.26	0.00006	$10^{49.5}$	3.2	$10^{17.7}$	$10^{14.7}$	$10^{14.2}$
FSRQ 1641+399	$10^{45.4}$	$10^{43.6}$	$10^{7.8}$	0.31	0.00004	$10^{47.7}$	1.2	$10^{17.2}$	$10^{14.0}$	$10^{13.5}$
FSRQ 2128-123	$10^{46.2}$	$10^{42.8}$	$10^{8.8}$	0.25	0.00007	$10^{50.0}$	4.3	$10^{17.8}$	$10^{15.4}$	$10^{14.8}$
FSRQ 2251+158	$10^{45.3}$	$10^{44.2}$	$10^{7.7}$	0.31	0.00003	$10^{47.5}$	1.0	$10^{17.2}$	$10^{13.9}$	$10^{13.4}$
FSRQ 0923+392	$10^{46.3}$	$10^{43.5}$	$10^{8.8}$	0.25	0.00008	$10^{50.2}$	5.1	$10^{17.9}$	$10^{15.0}$	$10^{14.5}$
FSRQ 2135-147	$10^{46.0}$	$10^{43.7}$	$10^{8.5}$	0.25	0.00007	$10^{49.5}$	3.1	$10^{17.7}$	$10^{14.7}$	$10^{14.2}$
FSRQ1156+295	$10^{44.9}$	$10^{43.1}$	$10^{7.5}$	0.24	0.00003	$10^{46.7}$	0.5	$10^{16.9}$	$10^{13.6}$	$10^{13.1}$
FRSQ 1510-089	$10^{46.4}$	$10^{42.7}$	$10^{8.7}$	0.41	0.00005	$10^{49.8}$	5.5	$10^{17.9}$	$10^{14.8}$	$10^{14.3}$
FSRQ 1706+006	$10^{44.0}$	$10^{42.0}$	$10^{6.6}$	0.19	0.00002	$10^{44.8}$	0.12	$10^{16.3}$	$10^{12.8}$	$10^{12.3}$
FSRQ 1355-055	$10^{46.5}$	$10^{44.0}$	$10^{9.2}$	0.15	0.0002	$10^{51.2}$	6.82	$10^{18.0}$	$10^{15.4}$	$10^{14.9}$

APPENDIX II. MAGNETOSPHERIC ETERNALLY COLLAPSING OBJECTS (MECO)

In general relativity, preservation of the strong principle of equivalence (SPOE) requires that special relativity must hold locally for all time-like observers in all of spacetime. The existence of MECO is implied by the idea that Nature requires that the SPOE must be dynamically preserved everywhere in spacetime for the timelike world lines of massive particles or fluids under the influence of both gravitational and non-gravitational forces. Preservation of the SPOE requires that the frame of reference of the co-moving observer in the massive collapsing fluid must always be connected to the frame of reference of a stationary observer by special relativistic transformations with a physical 3-speed that is less than the speed of light (SLR06 and Landau & Lifshitz 1975).

Since the left-hand side of the Einstein equation cannot by itself dynamically enforce the preservation of the SPOE, it follows that for collapsing objects there must exist SPOE-preserving non-gravitational processes in nature which must always be included in the energy–momentum tensor on the right-hand side of the Einstein equation. It was in this manner that the general relativistic MECO solutions to the Einstein-Maxwell equations were discovered, as was shown in the published papers of Robertson and Leiter (2002 ,2003 ,2004), and developed in more detail in Appendices 1–10 of Schild et al. (2005). There it was shown that for a collapsing body, the structure and radiation transfer properties of the energy–momentum tensor on the right-hand side of the Einstein field equations, could describe a collapsing radiating object which contained equipartition magnetic fields that generated a highly redshifted Eddington limited secular collapse process. This collapse process was shown to preserve the SPOE by dynamically preventing trapped surfaces, that lead to event horizons, from forming. In Appendices 1–10 of Schild et al. (2005) it was shown that, by using the Einstein–Maxwell equations and quantum electrodynamics in the context of general relativistic plasma astrophysics, it was possible to virtually stop and maintain a slow (many Hubble times!), steady collapse of a compact physical plasma object outside of its Schwarzschild radius.

The non-gravitational force was Compton photon pressure generated by synchrotron radiation from an intrinsic equipartition magnetic dipole field contained within the compact object. The rate of collapse is controlled by

radiation at the local Eddington limit, but from a highly red shifted surface with an extremely small photon escape cone.

In Appendix 9 and 10 of Schild et al. (2005) it was shown that the equatorial poloidal magnetic field, associated with a locally Eddington limited secular rate of collapse of the exterior surface, was strong enough to spontaneously create bound electron-positron pairs in the surface plasma of the MECO which contribute to the general relativistic surface drift currents, within the pair dominated plasma at the MECO surface. These electron-positron drift currents on the MECO surface generate the magnetic fields which create the MECO's distantly observed intrinsic magnetic moment.

Within the context of the MECO's Eddington limited secular balance, the action of this QED pair production process was shown to be sufficient to stabilize the collapse rate of the MECO surface. For the collapsing, radiating pair dominated plasma associated with the MECO, the corresponding exterior solution to the Einstein equation is described by the time dependent Vaidya metric, where no coordinate transformation between MECO Vaidya metric and the black hole Kerr–Schild metric exists. Since the highly red shifted Eddington limited MECO Vaidya metric solutions preserve the SPOE they do not have event horizons and the MECO exhibit distantly observed slowly rotating intrinsic magnetic dipole moments which can interact with their surrounding accretion disk environments.

In this way the super massive MECO existing in the center of quasar Q0957 revealed itself by generating unique observable magnetic effects on the accretion disk environment (i.e. the Schild-Vakulik Structure discussed in (SLR06)) which observationally distinguished it from that of a central Black Hole.

Robertson, S., & Leiter, D. 2002, ApJ, 565, 447
Robertson, S., & Leiter, D. 2003, ApJ, 596, L203
Robertson, S., & Leiter, D. 2004, MNRAS, 350, 1391
Schild, R., Leiter, D., & Robertson, S. 2006, AJ, 132, 420 **(SLR06)**
Landau, L. D., & Lifshitz, E. M. 1975, Classical Theory of Fields (4th ed.;Oxford: Pergamon Press)
Schild, R., Leiter, D., & Robertson, S. 2005, arXiv astro-ph/0505518 **(Schild et. al (2005))**
Robertson, S., and Leiter, D. 2005, "The Magnetospheric Eternally Collapsing Object (MECO) Model of Galactic Black Hole Candidates and Active Galactic Nuclei", pp 1-45 (in New Directions in Black Hole Research, ed. P.V. Kreitler, Nova Science Publishers, Inc. ISBN 1-59454-460-3, novapublishers.com)
Livio, M., Oglivie, G.I., & Pringle, J.E. (1998) astro-ph/9809093
Chou, W, & Tajima, T., (1999) ApJ 513, 401